Magnetization profile in antiferromagnetically coupled recording media

Michael F. Toney[a)]
Stanford Synchrotron Radiation Laboratory, Stanford Linear Accelerator Center, Menlo Park, California 94025

Julie A. Borchers, Kevin V. O'Donovan,[b)] and Charles F. Majkrzak
NIST Center for Neutron Research, National Institute of Standards and Technology, 100 Bureau Drive, Stop 8562, Gaithersburg, Maryland 20899-8562

David T. Margulies and Eric E. Fullerton
San Jose Research Center, Hitachi Global Storage Technologies, 650 Harry Road, San Jose, California 95120

(Received 13 December 2004; accepted 7 March 2005; published online 15 April 2005)

We report polarized neutron reflectivity (PNR) studies of antiferromagnetically coupled (AFC) magnetic recording media with the aim of understanding how the two ferromagnetic layers switch magnetization direction. The PNR measurements were conducted at applied magnetic fields from near saturation to near the coercive field of the upper layer. From the PNR spectra, we obtain the magnetization profile of the AFC media. The results verify that the lower layer is aligned antiparallel to the magnetically hard upper layer in low fields. However, the magnetization of the upper layer shows an unexpected decrease as the lower layer reverses direction, which indicates that the interaction between the upper and lower layers is more complex than previously thought. © *2005 American Institute of Physics*. [DOI: 10.1063/1.1906300]

The areal density in magnetic recording disk drives has been increasing rapidly in the past decade. This has traditionally been accomplished with a scaling approach by reducing the magnetic media thickness and the bit size, while keeping the number of grains per bit approximately constant. As a result, the grain volumes have become so small that thermal degradation of the magnetic media is a now significant concern.[1,2] Recently, antiferromagnetically coupled (AFC) recording media were introduced to improve thermal stability at high recording densities[3,4] and are the present pathway to densities beyond about 100 Gbits/in^2.[5,6] AFC media are comprised of two granular, ferromagnetic layers separated by a thin Ru layer whose thickness is tuned to antiferromagnetically couple the layers together. These media have a lower net areal remanent magnetic moment density and are thermally more stable than equivalent single layer media.[3,4,7–10] Here, we describe polarized neutron reflectivity (PNR) measurements of the depth-resolved profile of the magnetization in AFC media. In contrast to previous studies that only measure the integrated magnetization, PNR allows us to distinguish the magnetization in each ferromagnetic layer. Our goal is to obtain a clearer picture of the reversal mechanisms in the thin lower layer and the thick upper recording layer.

The medium used in this study[11] was deposited onto a glass substrate with various seed and underlayers to give a strong $(11\bar{2}0)$ preferred orientation[12,13] and with a CNx protective surface film. The upper magnetic layer (layer F_U with areal remanent moment density Mr_Ut_U, where Mr is the remanent magnetization and the thickness $t \approx 120$ Å) was a $Co_{63}Pt_{11}Cr_{18}B_8$ alloy with nominal $Mr_Ut_U = 0.38$ memu/cm^2, while the lower magnetic layer (layer F_L with Mr_Lt_L and $t \approx 30$ Å) was a $Co_{86}Cr_{14}$ alloy with nominal $Mr_Lt_L = 0.17$ memu/cm^2. These were antiferromagnetically coupled via a 0.7 nm Ru layer. Figure 1(a) shows the major hysteresis loop for the AFC media (solid line). The arrows show the magnetization configuration of the layers at several points along the loop. At large applied fields, the AF coupling is overcome and the magnetization in the ferromagnetic layers is parallel to the field. As the field is reduced, the thinner, lower layer first reverses at $H = H_{ex}$ to become antiparallel to the thick, upper layer. As the field is further reversed, F_U switches and both layers are again parallel to the field. While this explanation of the magnetic reversal is

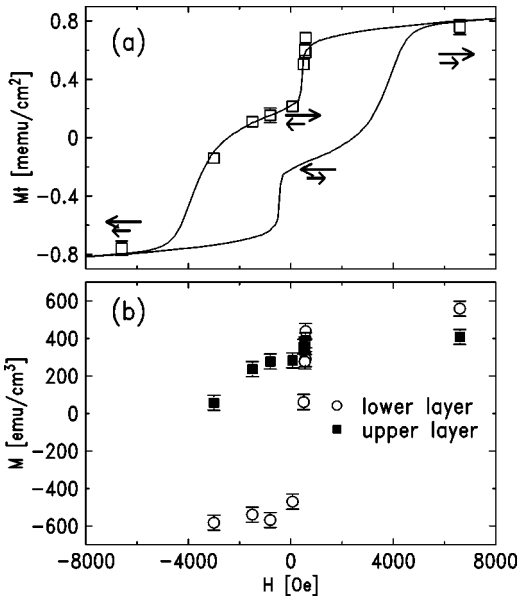

FIG. 1. (a) Magnetic hysteresis loop for AFC media. The solid line shows the SQUID areal magnetization density (Mt), while the open circles show PNR results. The arrows show the nominal magnetization configuration of the layers at several points. (b) Layer-resolved magnetization for upper layer (closed squares) and lower layer (open circles). In all cases, data were obtained with the applied field decreasing from saturation.

[a)]Electronic mail: mftoney@slac.stanford.edu
[b)]Also at University of California, Irvine, California.

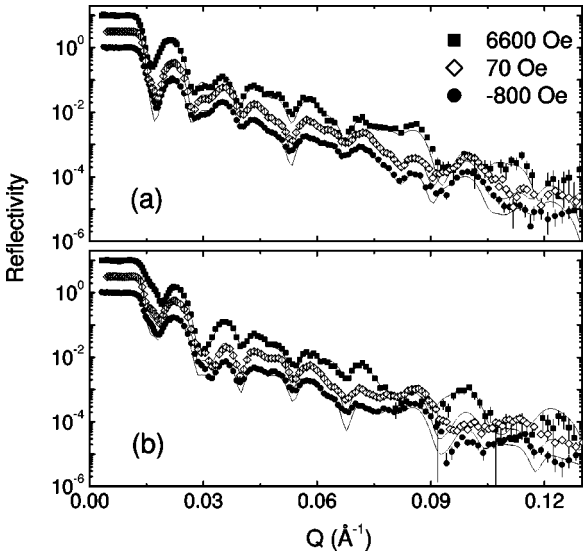

FIG. 2. PNR spectra at 6600, 70, and −800 Oe (squares, diamonds, and circles, respectively). (a) Parallel-parallel PNR, R(++). (b) Antiparallel-antiparallel PNR, R(−−). The spectra have been offset for clarity. Solid lines show the best fits to the data.

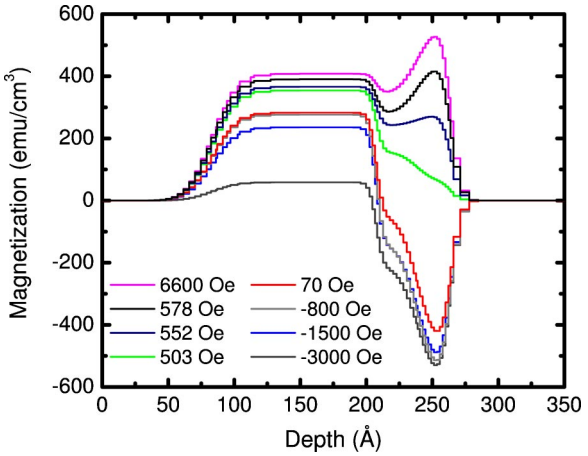

FIG. 3. Magnetization profile $M(z)$, where z is distance normal to the media surface and the origin is the top of the CNx layer. As the applied magnetic field decreases from 6600 to −3000 Oe, $M(z)$ decreases from top to bottom.

qualitatively correct, the specific behavior of the individual layers is often inferred from magnetization measurements of the composite system. The PNR measurements, which provide information about the depth dependence of the magnetization, give a more detailed understanding of the reversal process.

The PNR data were obtained at the NG-1 reflectometer at the NIST Center for Neutron Research at the National Institute of Standards and Technology (Gaithersburg, MD) using a neutron wavelength of 4.75 Å. The scattering plane was horizontal, and the neutrons were polarized in the vertical direction, in the plane of the thin film disk, using supermirror polarizers that select one of the neutron spin states. Typical polarization efficiencies exceeded 97%. The data were normalized and corrected for detector and polarizer efficiencies as described in Ref. 14. The diffuse background was subtracted from the data, and care was taken to ensure proper alignment of the disk sample. X-ray reflectivity data were obtained on a lab-based source using Cu K_{α_1}.[15]

We measured all four PNR reflectivities, R(++), R(−−), R(+−), and R(−+), where the + and − signs designate, respectively, parallel and antiparallel polarizations of the incident and reflected neutrons relative to the applied field. The R(++) and R(−−) nonspin flip reflectivities contain contributions from both the chemical film structure and the component of the magnetization along the applied field. Specifically, the difference in R(++) and R(−−) is directly related to the parallel magnetization component. The spin flip reflectivities R(+−) and R(−+) depend on the component of magnetization perpendicular to the field direction.[14] For all applied fields, these vanished for our AFC sample; hence, as expected, there is no magnetization component perpendicular to the field.

The squares, diamonds, and circles in Figs. 2(a) and 2(b) show, respectively, R(++) and R(−−) at applied magnetic fields of 6600, 70, and −800 Oe. As is apparent, there is an applied field dependence to both R(++) and R(−−) (e.g., see near 0.04 and 0.08 Å^{-1}) and these are different from each other (e.g., see near 0.03 and 0.08 Å^{-1}). These PNR spectra were fit using a modification of the Parratt formalism as described in Refs. 16,17. It is the overall agreement between the PNR spectra and the fit that is important in the data analysis. As a starting point to the fitting, x-ray reflectivity was used to obtain layer thicknesses, electron densities, and interfacial physical roughnesses, which were used as input for the refinement of the PNR data. Overall the agreement between the structural parameters obtained by refinement of the x-ray and neutron data is quite good. The best fits to the neutron data are shown by solid lines in Fig. 2 and model the data well.

Before discussing the results of the modeling, it is important to note that the PNR and x-ray reflectivity methods average laterally over the in-plane instrumental coherence length, 100 and 2 μm, respectively. Hence, physical roughness across the sample plane will tend to smear the layers together on average, and very thin layers (e.g., the Ru coupling layer) will not be distinct. Figure 3 shows the magnetization profiles $M(z)$ obtained from the best fits to the data (solid lines in Fig. 2); here z is the distance normal to the media surface with positive into the media, and the origin is arbitrarily set as the top of the CNx layer. Each layer is modeled as a square wave with the interface region described by an error function to account for interfacial roughness. The Ru layer is at about 220 Å and the apparent nonzero magnetization on this layer is due to the roughness effect described above. These depth-dependent magnetic profiles constitute the major result of these experiments, and have not been reported for AFC media before.

From these magnetization profiles (Fig. 3), we can first extract the net areal magnetic moment density, which is the integral of the magnetization times total media thickness. These values can be directly compared to the superconducting quantum interference device (SQUID) data. These are shown in Fig. 1(a), where the line is the SQUID data and the squares are from the PNR. As is apparent, there is excellent agreement, which provides confidence in the PNR results for the individual magnetic layers. In similar comparisons between PNR and other bulk magnetometry methods, good agreement has also been found.[18,19]

Focusing on the behavior of the individual magnetic layers in Fig. 3, the magnetization of the upper and lower layers is shown in Fig. 1(b). The plotted values correspond to the

amplitude of the square wave that describes each layer (see Fig. 3). We note that the reflectivity fits are quite sensitive to these individual layer moments. As is apparent, the magnetization of the CoCr alloy lower layer [open circles in Fig. 1(b)] reverses sharply at $H_{ex} \approx 500$ Oe. This is consistent with the behavior expected for an CoCr layer with intergranular exchange coupling.[9] The reversal further verifies the antiparallel alignment of the upper and lower layers in low fields.

For the upper CoPtCrB layer, the magnetization is shown by the closed squares in Fig. 1(b). Interestingly, we observe that as the applied field is reduced from 6600 Oe to approximately 580 Oe, M_U remains relatively flat at $Ms_U = 400$ emu/cm^3. However, near the reversal field for the lower layer ($H_{ex} \approx 500$ Oe), the magnetization of the upper layer abruptly drops to approximately 300 emu/cm^3, and then **gradually** decreases as the field is decreased to −3000 Oe. The drop near H_{ex} is surprising because the magnetization of the upper layer (which has magnetically decoupled grains and high anisotropy) is expected to decrease gradually through this entire field range. Instead, our results indicate that the magnetic state of the upper layer is influenced by the magnetic state of the lower layer during its reversal in a way that is not expected from simple models. We note that similar effects have been reported for a $Co_{84}Fe_{16}/Cr/Co_{75}Pt_{12}Cr_{13}$ trilayer in which the magnetic layers are nominally uncoupled.[20] In this case, the reduction of the magnetic moment of the hard $Co_{75}Pt_{12}Cr_{13}$ layer was attributed to stray magnetic fields in this layer produced by domain walls that form within the thin soft $Co_{84}Fe_{16}$ layer as it switches. During reversal of the lower layer in our AFC sample, it is possible that the lower layer forms domain walls that create comparable stray fields that compete with the antiferromagnetic coupling to the upper layer. This model is particularly applicable to our sample where the lower layer has relatively high intergranular exchange coupling compared to the upper layer and reversal by domain wall motion is likely. In general, the unexpected moment reduction indicates the process for writing data on the AFC media is more complicated than previously thought. We note, however, that this effect may be less pronounced in media which utilize thinner lower layers that are more strongly superparamagnetic.[7,9,10] The effect may also be less pronounced during recording where fields are locally applied and the lower layer is not expected to reverse by domain wall propagation.

To confirm the results above, we determined the areal magnetization density for both the upper and lower layers from $M(z)$ in Fig. 3. These areal densities are different from the (volume) magnetization and were calculated as the integral of $M(z)$ from $-\infty$ to 215 Å and 215 Å to $+\infty$ for the lower and upper layers, respectively. The midpoint of 215 Å is chosen as the middle of the Ru spacer layer [minimum of $M(z)$ for 6600 Oe], but the precise choice for this limit does not significantly affect resultant areal magnetization density. The behavior of the upper and lower layer areal magnetization densities are consistent with the upper and lower layer magnetization shown in Fig. 1(b), supporting our conclusion of a drop in the upper layer magnetization near H_{ex}. Furthermore, we find remanent lower and upper layer areal magnetization densities of 0.17 ± 0.03 and 0.33 ± 0.03 memu/cm^2, in good agreement with the nominal values (0.17 and 0.38 memu/cm^2, respectively).

In summary, we have used PNR to obtain the magnetization profile for AFC magnetic recording media, permitting us to distinguish the magnetization in each layer. We find good agreement between the net areal remanent magnetization density determined from PNR and SQUID, providing confidence in our depth-dependent results. The PNR data show that the field dependence of the magnetization of the lower layer is consistent with that expected for a layer with intergranular exchange coupling. The field dependence of the upper layer magnetization during reversal of the lower layer does not follow simple expectations for a layer with magnetically decoupled grains and high anisotropy that is antiferromagnetically coupled to the lower layer, but instead shows an abrupt reduction at H_{ex}. The coupling of the upper and lower layers during reversal may thus be more complex than previously assumed and may include interactions from domain walls in the lower layer.

Portions of this research were carried out at the Stanford Synchrotron Radiation Laboratory, a user facility operated by Stanford University on behalf of the U.S. Department of Energy, Office of Basic Energy Sciences.

[1] D. Weller and A. Moser, IEEE Trans. Magn. **35**, 4549 (1999).
[2] S. H. Charap, P. L. Lu, and Y. He, IEEE Trans. Magn. **33**, 978 (1997).
[3] E. E. Fullerton, D. T. Margulies, M. E. Schabes, M. Carey, B. Gurney, A. Moser, M. Best, G. Zeltzer, K. Rubin, H. Rosen, and M. Doerner, Appl. Phys. Lett. **77**, 3806 (2000).
[4] E. N. Abarra, A. Inomata, I. Okamoto, and Y. Mizoshita, Appl. Phys. Lett. **77**, 2581 (2000).
[5] B. R. Acharya, E. N. Abarra, A. Inomata, A. Ajan, and S. Shinohara, IEEE Trans. Magn. **39**, 645 (2003).
[6] B. R. Acharya, A. Inomata, E. N. Abarra, A. Ajan, D. Hasegawa, and I. Okamoto, J. Magn. Magn. Mater. **260**, 261 (2003).
[7] J. Lohau, A. Moser, D. T. Margulies, E. E. Fullerton, and M. E. Schabes, Appl. Phys. Lett. **78**, 2748 (2001).
[8] B. R. Acharya, A. Ajan, E. N. Abarra, A. Inomata, and I. Okamoto, Appl. Phys. Lett. **80**, 85 (2002).
[9] D. Margulies, A. Berger, A. Moser, M. E. Schabes, and E. Fullerton, Appl. Phys. Lett. **82**, 3701 (2003).
[10] E. E. Fullerton, D. T. Margulies, N. Supper, H. Doa, M. E. Schabes, A. Berger, and A. Moser, IEEE Trans. Magn. **39**, 639 (2003).
[11] D. Margulies, A. Moser, M. E. Schabes, and E. Fullerton, Appl. Phys. Lett. **81**, 4631 (2002).
[12] M. F. Doerner, X. Bian, M. Madison, K. Tang, Q. Peng, A. Polcyn, T. Arnoldussen, M. F. Toney, M. Mirzamaani, K. Takano, E. E. Fullerton, D. Margulies, M. Schabes, K. Rubin, M. Pinarbasi, S. Yuan, M. Parker, and D. Weller, IEEE Trans. Magn. **37**, 1052 (2001).
[13] M. F. Toney, E. E. Marinero, M. F. Doerner, and P. M. Rice, J. Appl. Phys. **94**, 4018 (2003).
[14] C. F. Majkrzak, Physica B **221B**, 342 (1996).
[15] M. F. Toney, C. M. Mate, K. A. Leach, and D. Pocker, J. Colloid Interface Sci. **225**, 119 (2000).
[16] C. F. Majkrzak and N. F. Berk, Phys. Rev. B **58**, 15416 (1998).
[17] J. F. Ankner and G. P. Felcher, J. Magn. Magn. Mater. **200**, 741 (1999).
[18] J. A. C. Bland, J. Vac. Sci. Technol. A **15**, 1759 (1997).
[19] S. Hope, J. Lee, G. Lauhoff, J. A. C. Bland, A. Eecole, D. Bucknall, J. Penfold, H. J. Lauter, V. Lauter, and R. Cubitt, Phys. Rev. B **55**, 11422 (1997).
[20] L. Thomas, J. Luning, A. Scholl, F. Nolting, S. Anders, J. Stohr, and S. Parkin, Phys. Rev. Lett. **84**, 3462 (2000).